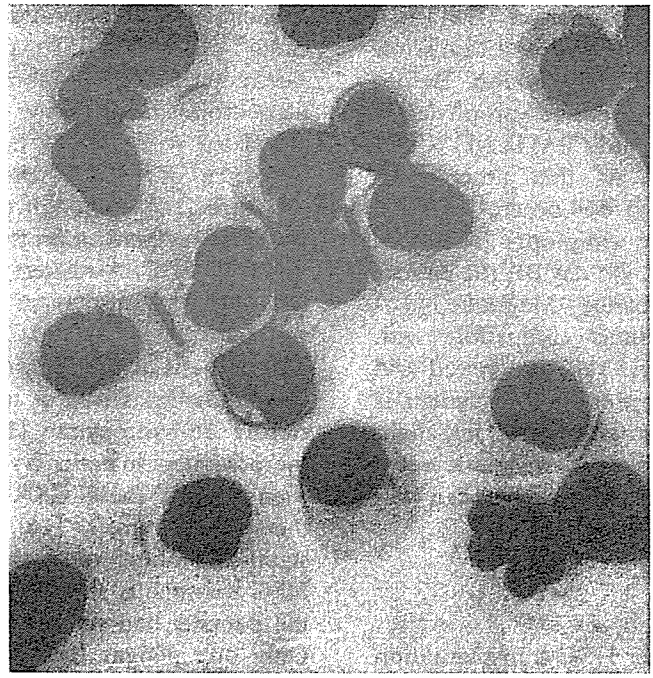

Figure 2. Cell morphology in CSF pleocytosis. Most cells were normal lymphocytes.

lymphocyte morphology, i.e. condensed round to oval nuclei without nucleoli and fine pale cytoplasm with a few azurophilic granules. CMV anti-genemia was detected in 10 patients receiving allogeneic HSC transplants but not in patients receiving autologous HSC transplants. Transplant-related complications were observed in the allogeneic HSC transplantation group as follows: sepsis (one); hemorrhagic cystitis due to adenovirus (one); bronchiolitis obliterans organizing pneumonia (one) and pseudomembranous colitis (two). None of the patients receiving autologous HSC transplants showed severe transplant-related complications. There were no patients having meningitis or encephalitis in both groups.

In allogeneic HSC transplantation, factors associated with CSF pleocytosis were analysed: CMV anti-genemia, acute GVHD, chronic GVHD and calcineurin inhibitor (CSA vs FK506) were not related to CSF pleocytosis (data not shown). Because calcineurin inhibitor blood concentrations may be associated with neurologic complications, we investigated the correlation between CSF cell numbers and CSA or FK506 blood concentrations. As shown in Figure 3, there was a positive correlation between CSF cell numbers and CSA trough levels but not FK506 trough levels.

There were no patients showing severe neurologic symptoms such as severe headache, blindness, seizures, cerebellar ataxia and confusion at the end of the last intrathecal methotrexate injection in the allogeneic HSC transplantation group. Some patients with CSF pleocytosis showed slight neurologic

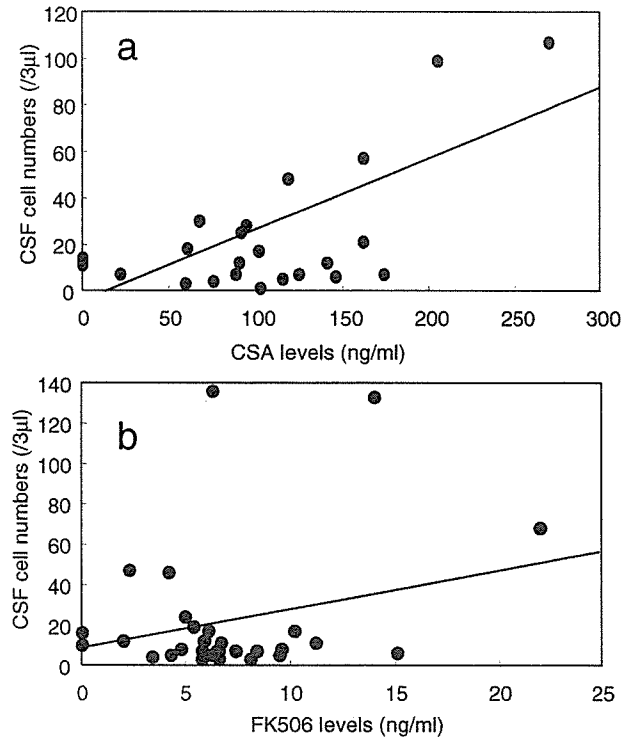

Figure 3. Relationship between CSF cell numbers and trough levels of calcineurin inhibitor. The numbers of analysed CSF samples were 24 in the CSA group and 31 in the FK506 group. CSF cell numbers correlated with CSA trough levels (a) $r^2 = 0.417$, $p = 0.0007$; but not with FK506 trough levels (b) $r^2 = 0.087$, $p = 0.1062$).

symptoms including tremor, nausea and headache at a mild level. Only one patient with lymphoblastic lymphoma developed leukoencephalopathy after

allogeneic bone marrow transplantation (BMT): a 15-year-old male who had been in second remission and had a history of meningeal infiltration. Before transplantation, the patient had received prophylactic cranial irradiation. On day 69 after BMT, MTX was injected intrathecally once. At this time, CSF pleocytosis (107 cells per 3 μl) was noted, although the patient had no neurologic symptoms. The CSA trough level was 270 ng ml^{-1}. On day 81, the patient complained of visual disturbance. Magnetic resonance imaging showed findings compatible with leukoencephalopathy. CSA was rapidly tapered and the symptom gradually disappeared. The patient is currently well without symptoms except for slight depression. Except for this patient, magnetic resonance imaging or computed tomography scan was not performed in other patients.

Discussion

Neurologic complications after HSC transplantation have been reported: these are caused by pre-transplant conditionings, metabolic disorders, viral infections, microangiopathy, complications induced by GVHD and calicineurin inhibitors [9,10]. de Brabander et al. [10] reported that severe neurologic complications are more frequent after BMT from alternative donors, compared with BMT for standard risk patients. They suggested that the increased incidence in alternative donor patients is associated with frequent lines of chemotherapy before BMT, intensified conditioning regimens including TBI and ATG used for the graft rejection prevention. The morbidity and profound immunosuppression caused by these treatments may lead to susceptibility to neurologic complications in patients receiving bone marrow transplants [10]. In our study, CSF pleocytosis was observed in allogeneic HSC transplantation but not in autologous HSC transplantation. Since TBI as conditioning and MTX as GVHD prophylaxis were used only in allogeneic HSC transplantation, these two treatments may have caused CSF pleocytosis in the patients [10–12]. In addition, unrelated donor HSC transplantation and ATG may have led to CSF pleocytosis associated with profound immunosuppression. Severe transplant-related complications occurred only in allogeneic HSC transplantation. Therefore, they may have been involved in CSF pleocytosis.

We suspect that CSF pleocytosis in allogeneic HSC transplantation may be associated with calcineurin inhibitors used for GVHD prophylaxis. Hauben [13] summarized neurotoxicity associated with CSA by the published literature: estimated the frequency of CSA neurotoxicity is 0.5–35% and risk factors of the toxicity include supratherapeutic blood concentrations of CSA, CSA-drug interactions and hypocholesterolemia. Associated abnormalities include elevated CSF protein and pleocytosis, electroencephalogram abnormalities and characteristic neuroimaging findings [13]. Similar neurotoxicity associated with FK506 has been reported and the incidence of the neurotoxicity is 5–30% in the literature [14], although the incidence and severity of FK506-related neurotoxicity are equal or higher than that of CSA-related neurotoxicity [4,15]. Postulated mechanisms of CSA neurotoxicity are vasculopathy based on CSA effects on endothelial cell synthesis of prostaglandin and release and uptake of endothelin as well as inhibition of mitochondrial steroid 26-hydroxylase [13]. CSA neurotoxicity is more frequent in patients with high CSA blood levels, even though these CSA levels are usually within therapeutic ranges [16]. We demonstrated that significant numbers of patients receiving allogeneic HSC transplants showed CSF pleocytosis and all of the patients had no or mild neurologic symptoms. Only one patient later developed leukoencephalopathy. These results suggest that CSF pleocytosis is relatively common in allogeneic transplantation and shows some brain damage. We observed a weak correlation between CSF cell numbers and CSA trough levels. Since CSA neurotoxicity is more frequent with high CSA blood levels [16], CSF cell numbers may reflect the degree of neurotoxicity. In contrast to CSA, there was no correlation between CSF cell numbers and FK506 trough levels. This may be due to the narrow therapeutic blood ranges of FK506. Since we did not measure CSA or FK506 concentrations in CSF, further studies are needed to identify a correlation between CSF cell numbers and calcineurin inhibitor concentrations in CSF. Although CSF pleocytosis is relatively common when allogeneic HSC transplantation is followed by calcineurin inhibitors for GVHD prophylaxis, we should carefully monitor such patients to detect early manifestations of leukoencephalopathy.

References

1. Woo M, Przepiorka D, Ippoliti C, Warkentin D, Khouri I, Fritsche H, Korbling M. Toxicities of tacrolimus and cyclosporin A after allogeneic blood stem cell transplantation. Bone Marrow Transplant 1997;20:1095–1098.
2. Reece DE, Frei-Lahr DA, Shepherd JD, Dorovini-Zis K, Gascoyne RD, Graeb DA, et al. Neurologic complications in allogeneic bone marrow transplant patients receiving cyclosporine. Bone Marrow Transplant 1991;8:393–401.
3. Stein DP, Lederman RJ, Vogt DP, Carey WD, Broughan TA. Neurological complications following liver transplantation. Ann Neurol 1992;31:644–649.
4. Mueller AR, Platz KP, Schattenfroh N, Bechstein WO, Christe W, Neuhaus, P. Neurotoxicity after orthotopic liver transplantation in cyclosporin A- and FK 506-treated patients. Transpl Int 1994;7(Suppl 1):S37–S42.

5. Bechstein WO. Neurotoxicity of calcineurin inhibitors: impact and clinical management. Transpl Int 2000;13:313–326.
6. Small SL, Fukui MB, Bramblett GT, Eidelman BH. Immunosuppression-induced leukoencephalopathy from tacrolimus (FK506). Ann Neurol 1996;40:575–580.
7. Faraci M, Lanino E, Dini G, Fondelli MP, Morreale G, Dallorso S, et al. Severe neurologic complications after hematopoietic stem cell transplantation in children. Neurology 2000;59:1895–1904.
8. Muroi K, Suzuki T, Amemiya Y, Yoshida M, Kawano C, Kuribara R, et al. Autologous peripheral blood stem cell transplantation for adults with B-lineage acute lymphoblastic leukemia: a pilot study. Leuk Lymphoma 2000;38:103–111.
9. Singh N, Paterson DL. Encephalitis caused by human herpesvirus-6 in transplant recipients: relevance of a novel neurotropic virus. Transplantation 2000;69:2474–2479.
10. de Brabander C, Cornelissen J, Smitt PA, Vecht CJ, van den Bent MJ. Increased incidence of neurological complications in patients receiving an allogenic bone marrow transplantation from alternative donors. J Neurol Neurosurg Psychiatr 2000;68:36–40.
11. van den Berg H, Gerritsen EJ, Haraldsson A, Vossen JM. Changes in cell and protein content of cerebrospinal fluid in children with acute lymphoblastic leukaemia after allogeneic bone marrow transplantation. Bone Marrow Transplant 1993; 12:615–619.
12. Rollins N, Winick N, Bash R, Booth T. Acute methotrexate neurotoxicity: findings on diffusion-weighted imaging and correlation with clinical outcome. Am J Neuroradiol 2004;25: 1688–1695.
13. Hauben, M. Cyclosporine neurotoxicity. Pharmacotherapy 1996;16:576–583.
14. Grimbert P, Azema C, Pastural M, Dhamane D, Remy P, Salomon L, et al. Tacrolimus (FK506)-induced severe and late encephalopathy in a renal transplant recipient. Nephrol Dial Transplant 1999;14:2489–2491.
15. Neuhaus P, McMaster P, Calne R, Pichlmayr R, Otto G, Williams R, et al. Neurological complications in the European multicentre study of FK 506 and cyclosporin in primary liver transplantation. Transpl Int 1994;7(Suppl 1):S27–S31.
16. Gijtenbeek JM, van den Bent MJ, Vecht CJ. Cyclosporine neurotoxicity: a review. J Neurol 1999;246:339–346.

Available online at www.sciencedirect.com
SCIENCE DIRECT®
Leukemia Research 30 (2006) 829–839
Leukemia Research
www.elsevier.com/locate/leukres

Establishment and characterization of a new erythroblastic leukemia cell line, EEB: Phosphatidylglucoside-mediated erythroid differentiation and apoptosis

Chizuru Kawano-Yamamoto [a], Kazuo Muroi [a,*], Yasuko Nagatsuka [b], Masato Higuchi [c], Satoru Kikuchi [a], Tadashi Nagai [a], Sen-itiroh Hakomori [d], Keiya Ozawa [a]

[a] *Division of Hematology, Department of Medicine, Jichi Medical School, Minamikawachi, Tochigi 329-0498, Japan*
[b] *Neural Circuit Mechanism Research Group, Brain Science Institute, RIKEN, Wako, Japan*
[c] *Fuji Gotemba Research Laboratories, Chugai Pharmaceutical Co., Gotemba, Japan*
[d] *Pacific Northwest Research Institute, Seattle, USA*

Received 23 March 2005; received in revised form 20 October 2005; accepted 22 October 2005
Available online 5 December 2005

Abstract

A new erythroblastic leukemia cell line (EEB) was established from a patient with early erythroblastic leukemia. The cells had features of immature erythroblasts, including an agranular basophilic cytoplasm and CD36, CD71, CD175s (sialyl-Tn) and CD235a (glycophorin A) expression without CD41 expression, myeloperoxidase activity and platelet-peroxidase activity. The cells were confirmed to be of the erythroid lineage based on expression of the gamma-globin message. They were induced to differentiate into benzidine-positive cells by hemin and δ-amino levulinic acid (δ-ALA). An analysis of cell membrane lipids showed that EEB cells contain a type of glycerolipid, phosphatidylglucose (PhGlc), but not unbranched type 2 chains, i antigens. GL-7 which is a recombinant Fab fragment of GL-2 and binds to PhGlc, induced production of hemoglobin F (HbF) associated with accumulation of the gamma-globin (γ-globin) message in EEB cells. The GL-7-mediated erythroid differentiation was associated with apoptosis. These results suggest that direct signaling to PhGlc mediates erythroid differentiation and apoptosis in EEB cells.

Keywords: Erythroid cell line; Phosphatidylglycoside; Differentiation; Apoptosis; Glycosphingolipid; Microdomain

1. Introduction

Blood cells express several types of carbohydrate antigens during the course of differentiation of hemopoietic progenitors. Roles of carbohydrates on myeloid cells have been studied extensively: sialyl-Lewis x (CD15s), which is a ligand of E-selectin on activated endothelial cells, is expressed in neutrophils [1]. The interaction between sialyl-Lewis x and E-selectin mediates tethering and rolling of neutrophils to the vessel wall in the microcirculation, although two other selectins also contribute to the adhesion and the transendothelial migration of neutrophils into tissues [1,2]. In erythroid cells, dramatic changes in carbohydrates associated with development have been reported: a progressive branching of lacto-*N*-glycosyl carbohydrate chains linked to glycolipids and to band 3 protein occurs during the development of fetal to adult human erythrocytes [3,4]. Some of the linear structure represents i antigen, while some of the branched structure represents i antigen. Such changes in carbohydrate structure in the membrane coincide with the switch from fetal hemoglobin to adult hemoglobin. Previously, we showed that sialyl-Tn is expressed in colony-forming unit-erythroid to erythroblasts but not in erythrocytes, while sialyl-T and disialy-T are expressed in the entire course of erythroid differentiation [5,6]. Although carbohydrate profiles in erythroid

* Corresponding author. Tel.: +81 285 58 7187; fax: +81 285 44 5087.
E-mail address: muroi-kz@jichi.ac.jp (K. Muroi).

0145-2126/$ – see front matter © 2005 Elsevier Ltd. All rights reserved.
doi:10.1016/j.leukres.2005.10.021

cells have been examined [7,8], little is known about the roles of carbohydrate antigens in erythroid cell differentiation. We established an erythroblastic leukemia cell line derived from a patient with early erythroblastic leukemia. Using this cell line, we found that erythroid differentiation and apoptosis are induced by GL-7, a recombinant Fab fragment reacting with PhGlc.

2. Materials and methods

2.1. Case history

The clinical course of the patient was previously reported [9]. A 49-years-old male was admitted to our hospital because of fever and gingival bleeding in November 1997. The peripheral blood showed a hemoglobin level of 7.3 g/dl, a platelet count of $2.6 \times 10^4\ \mu l^{-1}$, and a white blood cell count of $15{,}500\ \mu l^{-1}$ with 61% undifferentiated blasts. The serum lactate dehydrogenase level was markedly high (13,370 IU/l, normal <410 IU/l). A bone marrow aspirate demonstrated massive proliferation of blasts with undifferentiated features such as an extremely basophilic cytoplasm, a high nucleocytoplasmic ratio and one or more nucleoli. The blasts were negative for peroxidase, esterase (alpha-naphtyl butyrate and ASD-chloroacetate) and periodic acid-Schiff staining. Flow cytometry showed that the blasts were positive for CD36, CD71 and CD175s, but not for CD2, CD7, CD10, CD11b, CD13, CD15, CD19, CD33, CD34, CD41, CD45, CD38, CD235a or HLA-DR. The serum levels of sialyl-Tn and neuron-specific enolase activity were high. Karyotypic analysis of bone marrow cells showed 46,XY (37 cells/45 cells) and 47,XY,+8 (8 cells/45 cells). At first, the patient was suspected of having carcinocythemia of small cell carcinoma. Later, a final diagnosis of early erythroblastic leukemia was established based on the expression of the alpha-globin gene message. The patient died in December 1997 because of pulmonary bleeding after induction chemotherapy.

2.2. Cells and cell culture

Peripheral blood mononuclear cells were stored in a viable condition at −120 °C before the start of chemotherapy. Five months later, frozen peripheral blood mononuclear cells were thawed and cultured in YU-KLS medium, hormonally defined medium only containing 0.5% fetal calf serum (Yagai Research Center, Yamagata, Japan), supplemented with 10% fetal calf serum (FCS; Life Technologies Inc., Grand Island, NY) in 24-well plates at a concentration of $1 \times 10^6\ ml^{-1}$ at 37 °C in a 5% CO_2 incubator. After several weeks of culture, cells grew out and were maintained in the medium. To derive clones from the proliferating cells, single colonies grown in methylcellulose semi-solid media were picked up and cultured in the medium described above. A homogeneous population of cells was cloned by limiting dilution. The new erythroblastic leukemic cell line was designated EEB (early erythroblastic leukemia cell line) in October 1998.

The growth-supporting abilities of two hormonally defined media (STEMSPAN; StemCell Technologies, Inc., Vancouver, Canada, and EX-CELL Sp2/0, JRH Biosciences, Lenexa, KS) supplemented with 15% FCS and one standard medium (RPMI-1640; Invitrogen Co., Carlsbad, CA) supplemented with 15% FCS were examined. A polymerase chain reaction (PCR)-based method was used to test for contamination by mycoplasma and Epstein–Barr (EB) virus. Origins of the two types of cells were examined by Southern blot analysis.

CD34-positive cells were isolated by using the Mini-MACS CD34 isolation system (Miltenyi, Bergisch Gladbach, Germany) following the manufacturer's instructions. To obtain erythroblasts, clonal cell cultures were performed as follows: mononuclear cells were incubated in 1% methylcellulose, 30% fetal bovine serum, 1% bovine serum albumin, 3 U/ml erythropoietin, 50 ng/ml stem cell factor, 10 ng/ml granulocyte-macrophage colony-stimulating factor, 10 ng/ml interleukin-3, 10^{-4} M 2-mercaptoethanol and 2 mM L-glutamine (MethoCult GF H4434; StemCell Technologies Inc.). The cultures were incubated for 14 days at 37 °C in a 5% CO_2 incubator. On day 14 of culture, erythroid colonies were picked up and pooled.

2.3. Morphologic examination

Cells were stained with Wright–Giemsa, peroxidase, naphthol ASD-chloroacetate esterase, alpha-naphtyl butyrate esterase, acid phosphatase, Sudan black B and PAS solutions using standard methods. Hemoglobin-containing cells were detected using a specific reaction with benzidine/hydrogen peroxide solution (0.2% benzidine in 5 M glacial acetic acid and 10% H_2O_2) [10].

Electron microscopic examinations including analysis of morphology, platelet-peroxidase activity and myeloperoxidase activity, were described previously [11]. A platelet-peroxidase reaction was defined as positivity in the nuclear envelope and rough endoplasmic reticulum but negativity in the Golgi apparatus and cytoplasmic granules. A myeloperoxidase reaction was defined as positivity in the rough endoplasmic reticulum, nuclear envelope, Golgi apparatus and cytoplasmic granules.

2.4. Monoclonal antibodies

Commercially available fluorescein isothiocyanate (FITC) or phycoerythrin (PE)-conjugated monoclonal antibodies used for the cell surface marker analysis were as follows: CD3 (OKT3; Ortho Diagnostic Systems, Beers, Belgium), CD4 (T4; Coulter Immunology, Hialeah, FL), CD8 (T8; Coulter), CD10 (OKBcALLa; Ortho), CD11b (Leu15; Becton Dickinson Immunocytometry Systems, Mountain View, CA), CD13 (MY7; Coulter), CD14 (Mo2;

Coulter), CD15 (80H5; Immunotech, Marseille, France), CD19 (B4; Coulter), CD33 (MY9; Coulter), CD34 (HPCA-2; Becton), CD117 (NU-c-kit; Nichirei Co., Tokyo, Japan), CD41 (P2; Immunotech), CD45 (Becton), CD71 (Becton), CD235a (anti-glycophorin A; Immunotech), HLA-DR (OKDR; Ortho) and anti-HbF (IQ products; Groningen, The Netherlands). Anti-sialyl-Tn (CD175s; TKH2), anti-sialyl-T (QSH1) and anti-disialyl-T (QSH2) monoclonal antibodies that react with erythoid cells were reported previously [5,6]. The human IgM monoclonal antibody GL-2 was originally established as an anti-i antibody and subsequently shown to also react with PhGlc [12,13]. GL-7, a recombinant Fab fragment of GL-2, reacts only with PhGlc [14].

2.5. Antigen expression analysis

The method used for flow cytometric analysis was described previously [5,6,9]. Cells were incubated with FITC or PE-conjugated monoclonal antibodies for 30 min at 4 °C. Alternatively, cells were incubated with unconjugated monoclonal antibodies for 30 min at 4 °C and then FITC-conjugated anti-mouse or anti-human immunoglobulin for 30 min at 4 °C. Isotypic-matched antibodies were used as a negative control. The surface immunophenotype was assessed using a flow cytometer (Cytoron; Ortho Diagnostic Systems, Raritan, NJ). HbF content was evaluated using a previously reported method [15]. Briefly, cells were fixed by suspension in 1 ml of 4% paraformaldehyde (Sigma Chemical Co., St. Louis, MO) for 10 min at room temperature. The cells were permeabilized by resuspending them in a 1-ml mixture of methanol:acetone (1:4, v/v) for 1 min. A PE-conjugated anti-HbF monoclonal antibody was added, and the mixture was incubated for 45 min at room temperature. Isotypic-matched IgG was used as a negative control. Stained cells were analyzed using a flow cytometer (Cyto ACE-150, JASCO Co., Tokyo).

The method used for the evaluation of erythropoietin receptors was reported previously [16]. Cells were incubated with biotinylated erythropoietin or, as controls, with biotinylated erythropoietin plus a 1000-fold excess of unlabelled erythropoietin at 37 °C for 1 h. The cells were then incubated with 2 μg/ml of streptavidin-RED670 conjugate (SARED670; Gibco BRL, Brand Island, NY) at 4 °C for 1 h. Stained cells were analyzed using a flow cytometer (FACScan, Becton, Mansfield, MA).

For immunostaining [14], cells were fixed with 3% paraformaldehyde for 20 min at room temperature, quenched with 50 mM NH_4Cl, and then blocked with 0.2% gelatin. Cells were incubated overnight with GL-2 at 4 °C and then with FITC-conjugated anti-human IgM and Alexa 594-conjugated cholera toxin (Molecular Probes, Inc., Eugene, OR). Cells were examined with a Zeiss LSM 510 confocal microscope equipped with a Plan-Apochromat ×100 oil DIC objective.

2.6. Chromosomal analysis

Karyotypes were analyzed with a G-banding method [17]. Briefly, the cells were incubated with 0.02 μg/ml of colcemid (Gibco BRL) for 2 h for metaphase arrest. Hypotonic treatment was carried out with 0.075 M KCL for 20 min. The cells were fixed with methanol–acetic acid (3:1), dropped onto glass slides, and air-dried. Metaphases were analyzed.

Multicolor-fluorescence in situ hybridization (FISH) on metaphase preparations was performed using Spectra Vysion probes according to the instructions of the manufacturer (Vysis, Downers Grove, IL). Images were visualized by an epifluorescence microscope (Zeiss, Oberhochen, Germany) and analyzed using an Applied Imaging CytoVision Work station (Newcastle, UK). Ten metaphase cells were analyzed.

2.7. Effects of agents

Cells were suspended in YU-KLS medium containing 10% FCS at a concentration of 1×10^5 ml^{-1} and incubated for 4 days at 37 °C after the addition of appropriate concentrations of several agents. The inducers used were 1.0% dimethylsulfoxide (DMSO; Sigma), 1×10^{-3} M δ-ALA (Sigma), 1×10^{-6} M butyric acid (BA; Sigma), 1×10^{-4} M hydroxyurea (HU; Sigma), 1×10^{-10} M actinomicine-D (AD; Sigma), 1×10^{-4} M hemin (Sigma), 1×10^{-7} M cytosine arabinoside (Ara-C; Sigma), 1×10^{-6} M retinoic acid (RA; Sigma) and 5×10^{-6} M phorbol 12-myristate 13-acetate (PMA; Sigma). In negative controls, only buffer was added. In other experiments, cells (1×10^6 ml^{-1}) suspended in YU-KLS medium containing 10% FCS were treated with either 10 μg/ml, 100 μg/ml or 200 μg/ml of GL-7 for 4 days at 37 °C. In negative controls, 10 μg/ml of human IgM (Chemicon International, Temecula, CA) was added. In another set of experiments, the following commercially supplied cytokines were used: erythropoietin (EPO; 5 U/ml; Kirin Brewery Co., Tokyo, Japan), granulocyte colony-stimulating factor (G-CSF; 10 ng/ml; Chugai Pharmaceutical Co., Tokyo, Japan), granulocyte-macrophage colony-stimulating factor (GM-CSF; 10 ng/ml; Genzyme Diagnostics, Cambridge, MA), Interleukin-3 (IL-3; 10 ng/ml; Genzyme), IL-6 (5 ng/ml; R & D Systems), interferon-γ (IFN-γ; 10 U/ml; JCR Pharmaceutical Co., Kobe, Japan) and tumor necrosis factor-α (TNF-α; 10 ng/ml; Genzyme). Following treatment, erythroid differentiation and myeloid differentiation and apoptosis were evaluated.

2.8. Assessment of apoptosis

The apoptosis assay was carried out using a MEBCYTO apoptosis kit (MBL, Nagoya, Japan) according to the manufacturer's instructions [18]. In brief, cells were washed and resuspended in binding buffer. FITC-conjugated Annexin V and propidium iodide (PI) were added to the cell suspension, and then the mixture was incubated for

15 min in the dark at room temperature. Thereafter, the suspension was analyzed using a flow cytometer (FACScan, Becton).

2.9. Isolation of glycolipid and thin-layer chromatography (TLC) Immunostaining

Glycolipids were isolated from EEB cells as described previously [19]. The lipid extract was applied to a phenylboronate-agarose column (PBA-60, Millipore Co., Billerica, MA) and glycolipids were eluted with a chloroform/methanol/water (5:5:1, v/v/v) solution. For the isolation of GL-2-reactive lipids, TLC immunostaining was performed using GL-2 followed by horseradish peroxidase (HRP)-conjugated anti-human IgM [14]. The immunoreactive lipids were visualized using 3,3′-diaminobenzidine tetra hydrochloride (ICN Biochemical Inc., OH) as a chromogen [14].

2.10. Reverse transcription-polymerase chain reaction (RT-PCR)

RT-PCR was performed as described previously [20]. Briefly, cDNA was synthesized using 4 μg of total RNA extracted with the RNeasy Mini Kit (QIAGEN) and Superscript II reverse transcriptase (Invitrogen Co., Carlsbad, CA). cDNA was amplified in 25 μl of 10 mM Tris–HCl, 2.5 mM $MgCl_2$ and 50 mM KCl (pH 8.3). Taq DNA polymerase (Roche Diagnostics, Basel, Switzerland) was added at 1 U/reaction mixture. The PCR profile was as follows: denaturation for 30 s at 94 °C, annealing for 30 s at 55 °C and extension for 30 s at 72 °C (35 cycles). The reactions were run in a 9600R (Roche). The following primer sequences were used for reverse transcription-polymerase chain reaction: γ-globin forward primer, 5′-TGGCAAGAAGGTGCTGACTTC-3′; γ-globin reverse primer, 5′-TCACTCAGCTGGGCAAAGG-3′. These primers were purchased from Invitrogen.

2.11. Quantitative real-time PCR analysis

Quantitative real-time PCR analysis was performed as described previously [20]. Briefly, cDNA was synthesized using RNeasy Mini Kit-extracted (QIAGEN) total RNA, oligo(dT)12-18 primer and moloney murine leukemia virus reverse transcriptase (Invitrogen). PCR amplifications were performed in 25-μl reaction mixtures consisting of Taq Man Universal PCR Master Mix, No UNG (PE Biosystems, Warrington Cheshire, UK), 0.4 μM of the forward and reverse primers (Invitrogen), 0.25 μM of the TaqMan Probe (Applied Biosystems) and 5 μl of cDNA template. The PCR cycles were as follows: denaturation for 30 s at 94 °C, annealing for 30 s at 55 °C and extension for 30 s at 72 °C (50 cycles). The reactions were run in an ABI PRISM 7700 Sequence Detection system using the software Sequence Detection System Version 1.6.3 (PE Biosystems). The following primer and probe sequences were used for quantitative real-time PCR: γ-globin forward primer, 5′-TGGCAAGAAGGTGCTGACTTC-3′; γ-globin reverse primer, 5′-TCACTCAGCTGGGCAAAGG-3′; γ-globin probe, 5′-FAM-TGGGAGATGCCATAAAGCACCTGG-TAMRA-3′. The fluorescent reporter and the quencher were 6-carboxyfluorescein and 6-carboxy-*N,N,N′,N′*-tetramethylrhodamine, respectively. For quantitative real-time PCR of the reference genes, we used the endogenous control human glyceraldehyde-3-phosphate dehydrogenase Assays-on-Demand Gene Expression Products (Applied Biosystems).

2.12. Immunoblotting

Immunoblotting for tyrosine-phosphorylated protein was performed using HRP-conjugated PY20 (Transduction Laboratories, Lexington, KY) as described previously [21]. After the incubation of EEB cells (2×10^7 ml^{-1}) for 4 days, 50-μl aliquots were transferred to microtubes, and an equal volume of GL-7 (20 μg/ml) was added. After 10 min, stimulation was terminated by adding 50 μl of SDS sample buffer. For a control, cells were treated with an unrelated Fab antibody (anti-HBs). Protein tyrosine phosphorylation was assessed by immunoblotting using HRP-conjugated PY20.

3. Results

3.1. Establishment of a new erythroblastic leukemia cell line

The EEB cell line has been maintained in YU-KLS medium supplemented with 10% FCS for more than 6 years since the cell culture of leukemic cells from the patient started. EEB cells grow as single cells in suspension without adhering to plastic dishes. The growth of EEB cells showed an exponential growth phase, which was followed by a plateau phase. The doubling time was 38 h. No specific proliferation parameters were identified. For aggressive proliferation, the initial cell concentration required was more than 5×10^6 cells per ml. EEB cells can be frozen under standard conditions using 70% medium, 20% FCS and 10% dimethylsulfoxide (Cellbanker; Nippon Zenyaku Co., Koriyama, Japan) and thawed cells easily grow in the same medium. EEB cells remain stable during this culture period and also after freezing and thawing. The two hormonally defined media, STEMSPAN and EX-CELL, similarly supported the growth of EEB cells, while the standard medium, RPMI-1640, hardly supported the growth of the cells (data not shown). Mycoplasma and EB virus were not detected in EEB cells. Southern blot analysis of genomic DNA extracted from EEB cells and the patient's leukemic cells showed the same bands, which suggested that EEB cells are derived from the patient's leukemic cells (data not shown). The DNA fingerprint analysis was planned to perform to exclude cell contamination in EEB cells later, however, it was impossible because original leukemic cells from the patient was no longer left.

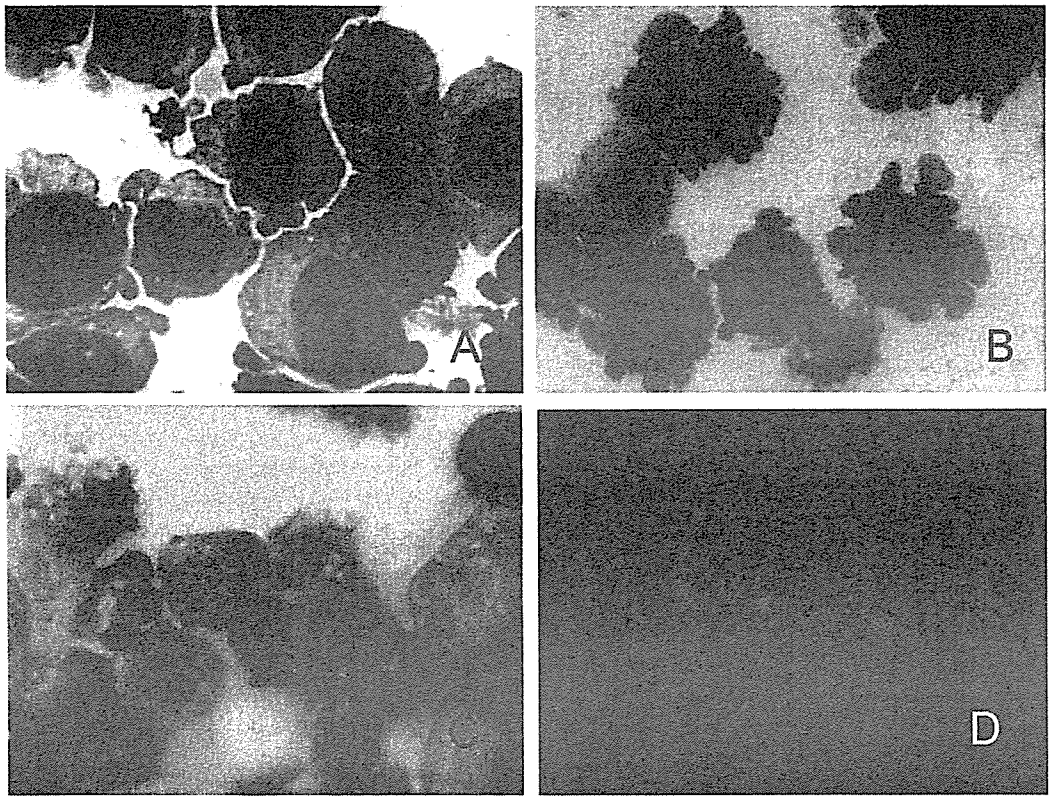

Fig. 1. Morphologic examination of EEB cells. EEB cells were immature erythroblastic cells (A) and showed a decrease in cell size and nuclear condensation after treatment with GL-7 at a concentration of 100 μg/ml for 2 days (B), while most underwent apoptosis after treatment with GL-7 at 200 μg/ml for 3 days (C). EEB cells were positively stained with GL-2 (D). (A–C) Wright–Giemsa staining; (D) immunostaining.

3.2. Morphologic analysis

EEB cells were medium to large and had round-shaped nuclei with several nucleoli and a basophilic agranular cytoplasm (Fig. 1A). The cells were negative for peroxidase, alpha-naphthyl butyrate esterase, naphthol-ASD-chloroacetae, Sudan black B and PAS stainings. A small percentage of the cells were positive for acid phosphatase staining. These features resemble those of the patient's leukemic blasts and immature erythroblasts. Although the original leukemic cells of the patient showed positive staining for neuron-specific enlolase activity, EEB cells had lost the activity (data not shown). The ultrastructural study showed that EEB cells had immature blastic features without myeloperoxidase activity, platelet-peroxidase activity or granules containing ferritin molecules (data not shown).

3.3. Immunophenotypic analysis

The cell surface marker profiles are summarized in Table 1. The surface markers of the EEB cells were almost the same as those of the original blasts. EEB cells were only positive for CD36, CD45, CD71, CD117, CD235a, and erythroid-associated carbohydrate antigens, including sialyl-T, disialyl-T and CD175s, at various expression levels. The cells were negative for myeloid antigens, including CD13, CD15 and

Table 1
Phenotypic characteristics

Antigen (CD)	EEB (%)	Patient (%)
CD2	0.5	0.8
CD3	0.4	ND
CD7	0.4	1.8
CD10	0.4	0.2
CD11b	0.5	12.7
CD13	0.8	14.4
CD15	1.6	4.4
CD19	0.3	5.2
CD20	1.0	11.6
CD33	11.7	8.0
CD34	0.2	1.5
CD36	99.9	99.9
CD41	0.8	0.8
CD45	97.0	13.9
CD71	48.7	77.3
CD117	36.4	ND
CD175s	88.8	88.8
CD235a	72.1	8.4
HLA-DR	0.5	6.4
Sialyl-T	95.3	87.0
Disialyl-T	35.6	41.0
GL-2	56.0	ND

CD175s, sialyl-Tn; CD235a, glycophorin A; ND, not determined. The values of EEB cells shown are the percent positive cells of representative data in three tests. Reactivity is defined as positive when more than 15% of cells are stained with a monoclonal antibody.

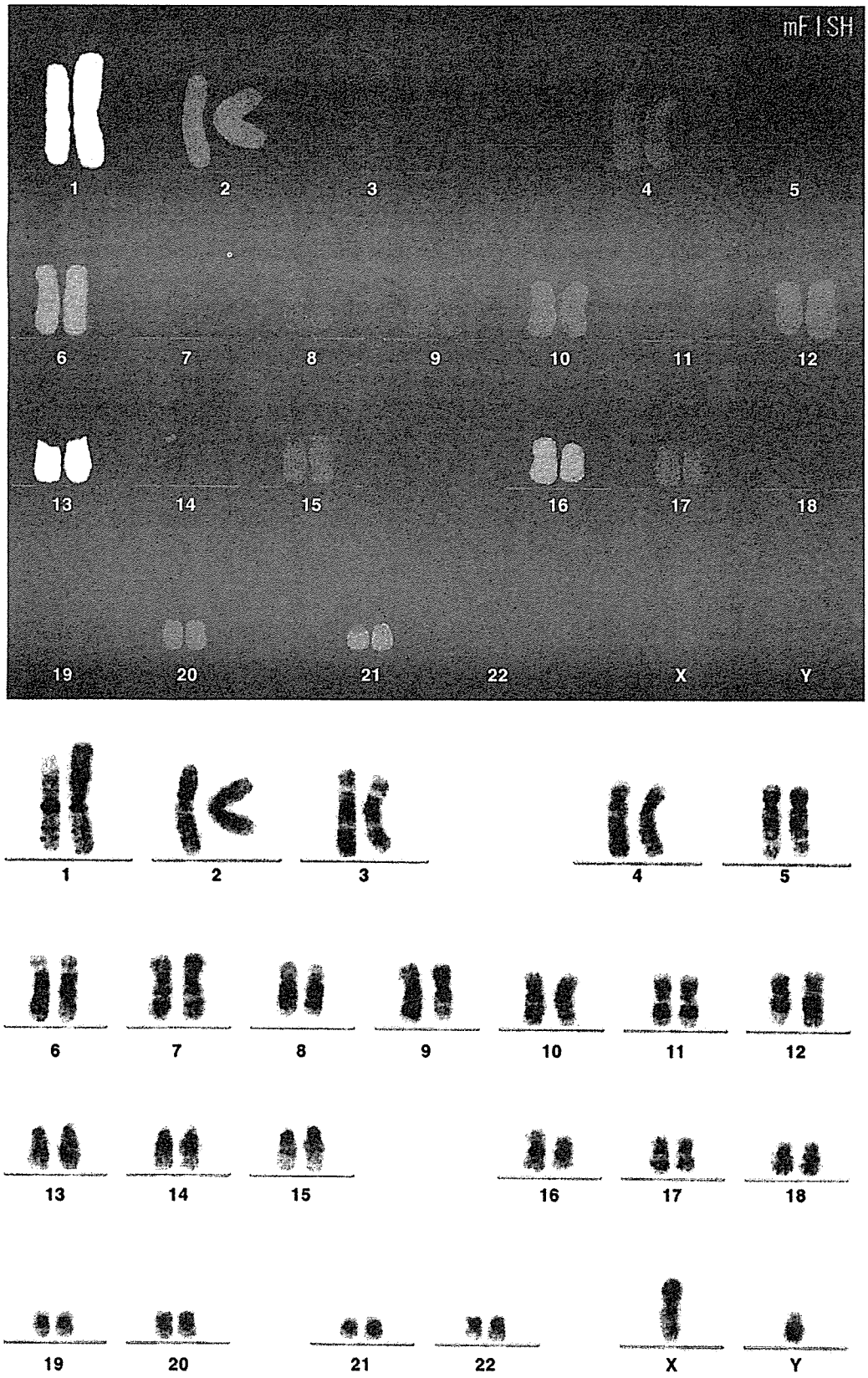

Fig. 2. Multicolor FISH analysis. EEB cells showed a normal karyotype.

CD33, lymphoid antigens, including CD2, CD3, CD7, CD10, CD19 and CD20, a stem cell antigen (CD34), and a platelet antigen (CD41). The cell surface antigen expression profiles showed that EEB cells belong to an erythroid lineage and are more differentiated than the original blasts. Erythropoietin receptor expression was analyzed using flow cytometry; EEB cells did not express erythropoietin receptors even though they were treated with PMA or DMSO (data not shown). Using this method, erythropoietin receptor expression was shown in an erythropoietin-responsive erythroid cell line, AS-E2 [22].

The flow cytometric analysis showed that about 56% of the EEB cells expressed an antigen(s) recognized by GL-2 (Table 1). Reactivity of the antibody with EEB cells was also confirmed using immunostaining: the membrane reaction was clustered showing a capping-like phenomenon (Fig. 1D).

3.4. Cytogenetic analysis

A chromosomal analysis of G-banding metaphases of EEB cells was performed three times, i.e., 1, 2 and 3 years after the establishment; EEB cells revealed that the karyotype was normal, 46,XY in all analyses (Fig. 2). The normal karyotype of EEB cells was confirmed by the multicolor FISH analysis; all 10 of the cells analyzed showed 46,XY (Fig. 2). EEB cells showed no p53 gene mutation, tandem duplication of the FLT3 gene, or FLT3 activation loop mutation (data not shown).

3.5. Induction of differentiation

Benzidine-positive cells were counted after EEB cells had been treated with hemin, DMSO, δ-ALA, BA, HU, AD, hemin and Ara-C (Fig. 3). Untreated EEB cells were negative for the hemoglobin staining, while 40–50% of the cells treated with δ-ALA or hemine were positive for benzidine. After incubation with PMA, EEB cells loosely adhered to plastic dishes and exhibited a decrease in cytoplasmic basophilia. However, no cytochemical change, including alpha-naphthyl butyrate esterase activity or change in the expression of surface antigens (CD11b, CD13, CD14, CD15, CD33, CD36, CD41 and CD235a) was observed (data not shown). Similarly, RA did not obviously induce myeloid or erythroid differentiation of EEB cells (data not shown).

Since GL-7 induces granulocytic differentiation of HL-60 cells [14], the effect of the Fab fragment on EEB cell differentiation was examined. As shown in Fig. 4A, GL-7 inhibited the growth of EEB cells in a dose-dependent manner. The growth inhibition induced by GL-7 was associated with erythroid differentiation and apoptosis. Following treatment of EEB cells with GL-7, the number of benzidine-positive cells increased: maximal erythroid differentiation occurred after a 2-day incubation with the addition of 100 μg/ml of GL-7 (Fig. 4B). In this setting, EEB cells showed a decrease in both cell size and cytoplasmic basophilia, and nuclear condensation (Fig. 1B). An increase in the production of HbF was

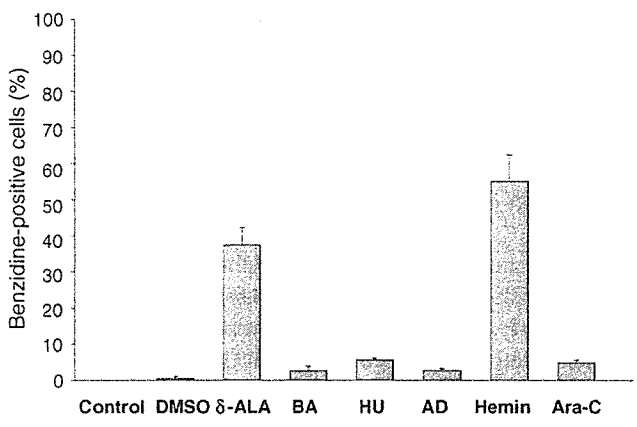

Fig. 3. Differentiation to benzidine-positive cells induced by various agents. EEB cells were cultured with DMSO, δ-ALA, BA, HU, AD, hemine, Ara-C and GL-7 at appropriate concentrations for 4 days. After incubation, benzidine-positive cells were counted. The addition of δ-ALA and hemin induced EEB cells to differentiate into benzidine-positive cells. Each value is the mean ± S.D. of three experiments conducted in duplicate.

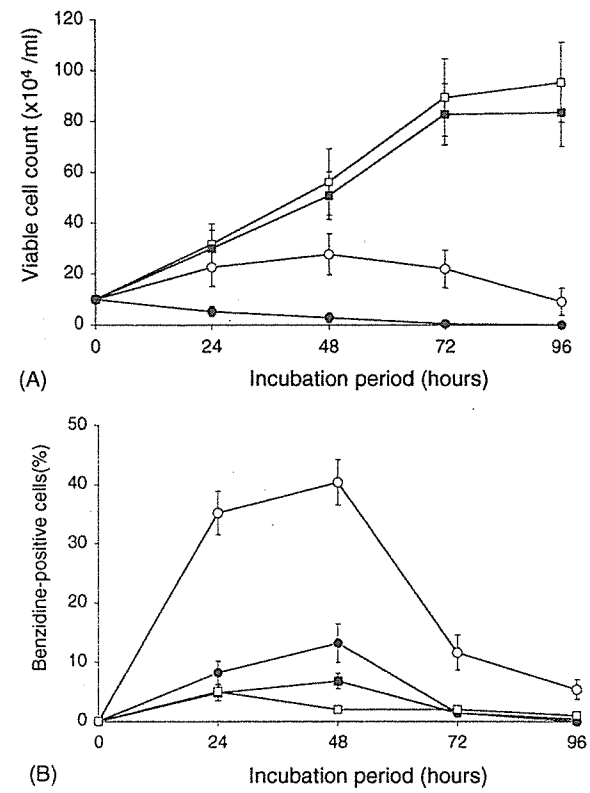

Fig. 4. Growth curve of EEB cells and differentiation to benzidine-positive cells induced by GL-7. Viable cells were counted following treatment of EEB cells with GL-7 or no treatment (A). (□) Control (human IgM); (■) 10 μg/ml of GL-7; (○) 100 μg/ml of GL-7; (●) 200 μg/ml of GL-7. Each value is the mean ± S.D. of three experiments conducted in triplicate. GL-7 induced the differentiation into benzidine-positive EEB cells in a dose-dependent and a time-dependent manner (B): maximal numbers of benzidine-positive cells were observed on treatment with 100 μg/ml of GL-7 for 2 days. (□) Control (human IgM); (■) 10 μg/ml of GL-7; (○) 100 μg/ml of GL-7; (●) 200 μg/ml of GL-7. Each value is the mean ± S.D. of three experiments conducted in triplicate.

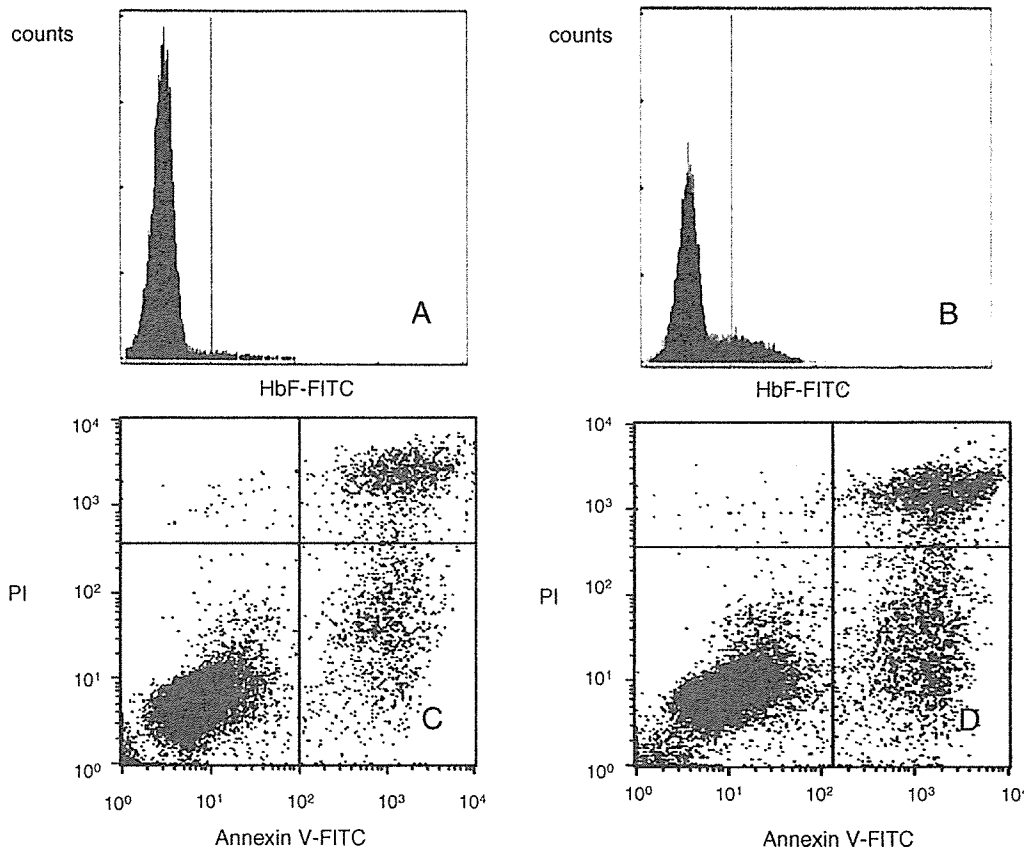

Fig. 5. Production of HbF and apoptosis induced by GL-7. The addition of 100 μg/ml of GL-7 for 2 days induced production of HbF in EEB cells (B) compared with the addition of control human IgM (A). However, the addition of 100 μg/ml of GL-7 for 3 days increased the number of apoptotic cells (D) compared with the addition of control human IgM (C). One representative experiment of three performed.

confirmed to have occurred using flow cytometry (Fig. 5B). The induction of erythroid differentiation of EEB cells by GL-7 was associated with apoptosis. The apoptosis induced by GL-7 was confirmed based on morphologic changes: EEB cells showed cytoplasmic membrane blebbing and nuclear fragmentation (Fig. 1C). GL-7-induced apoptosis was confirmed using flow cytometry utilizing Annexin V and PI staining (Fig. 5D). Following treatment with GL-7, the number of apoptotic cells increased: on the addition of 100 μg/ml of GL-7, apoptotic cells numbers increased after maximal erythroid differentiation on day 2 of the culture (Fig. 4A). In contrast, the addition of 200 μg/ml of GL-7 for 3 days caused the apoptosis of most cells with minimal erythroid differentiation (Figs. 1C and 4B).

GM-CSF and IL-6 slightly stimulated only the growth of EEB cells (145% and 150% versus 100% of control without cytokine-stimulation, respectively), while other cytokines including EPO, G-CSF, IL-3, IFN-γ and TNF-α did not affect the growth or the differentiation (data not shown).

3.6. Analysis of γ-globin message

The γ-globin message was detected by RT-PCR (Fig. 6A). EEB cells treated with GL-7 expressed the message. Because untreated EEB cells also expressed it, a quantitative real-time PCR analysis was conducted to identify induction of the γ-globin message in EEB cells treated with GL-7. As shown in Fig. 6B, GL-7-treated EEB cells showed a slight increase in γ-globin message content.

3.7. Analysis of PhGlc in EEB cells

GL-2 reacts with two carbohydrates, i and PhGlc [13]. Therefore, carbohydrate profiles of the EEB cell membrane were analyzed using TLC immunostaining: PhGLc but not i was detected in the EEB cell membrane (Fig. 7).

3.8. Analysis of phosphorylation

To determine whether the erythroid differentiation induced by GL-7 is associated with protein tyrosine phosphorylation, early changes in protein tyrosine phosphorylation were analyzed. EEB cells treated with GL-7 showed no protein tyrosine phosphorylation (data not shown).

3.9. Expression profiles of GL-2-reactive blood cells

Profiles of i and PhGlc expression in normal blood cells are not well understood. Therefore, the reactivity of GL-2 with various blood cells was examined: GL-2 reacted with

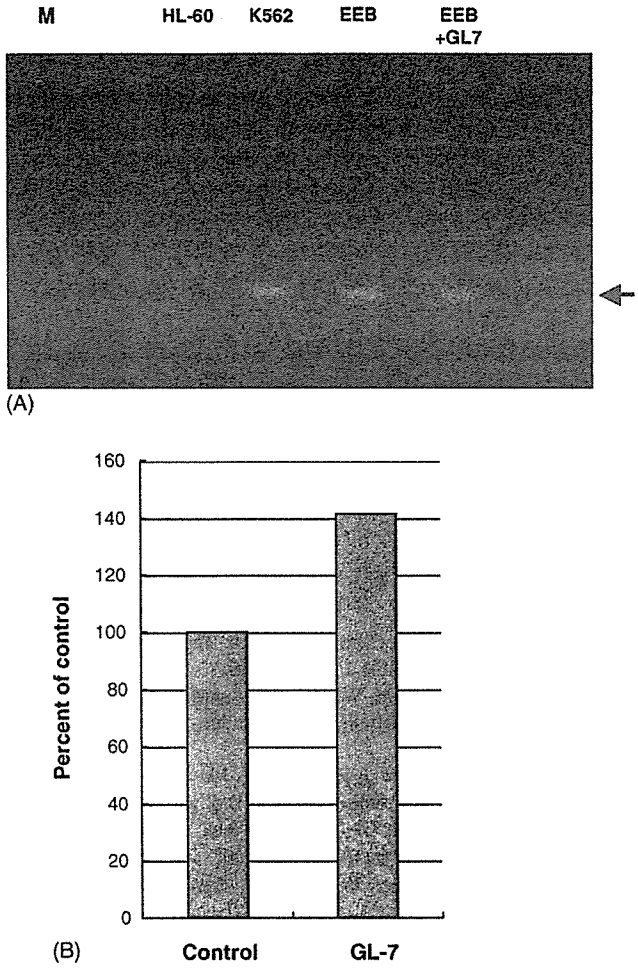

Fig. 6. Assessment of γ-globin gene expression in EEB cells. The γ-globin message was detected in K562 cells and in EEB cells treated or not treated with GL-7 but not in HL-60 cells by RT-PCR analysis (A). Quantitative RT-PCR analysis showed a slight increase in the γ-globin message in EEB cells treated with GL-7 for 48 h compared with cells treated with control human IgM for 48 h (B). One representative experiment of two performed.

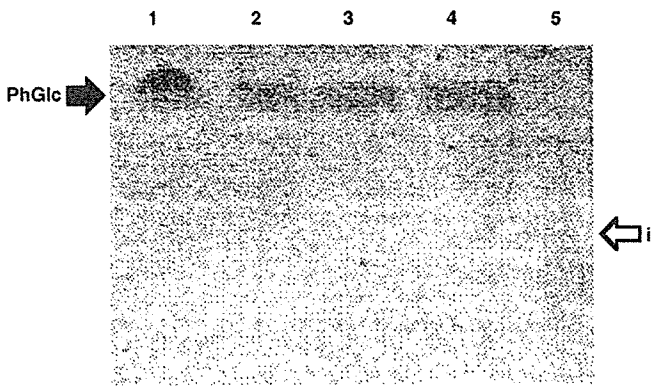

Fig. 7. TLC immunostaining. Lanes 1–5 indicate the application of 8 μl of PhGlc, 1 μl, 2 μl and 4 μl of glycolipid extracted from EEB cells, and 8 μl of i glycolipid, respectively. EEB cells contain PhGLc (the black arrow, the narrow band) but not i glycolipid (the white arrow, the wide band). One representative experiment of two performed.

cord blood erythrocytes (42%) and erythroblasts derived from both adult bone marrow (36%) and cord blood (64%) but not with CD34-positive cells (1%) or adult erythrocytes (1%).

4. Discussion

We established a human erythroblastic leukemia cell line, EEB, from a patient with early erythroblastic leukemia. Morphologic, cytochemical, immunophenotypic and gene expression analyses demonstrated that EEB has features of immature erythroid cells, including expression of CD36, CD71, CD175s, CD235, HbF and γ-globin message. Erythropoietin receptors were not detected in EEB cells, but that is not surprising. Generally, erythropoietin-independent erythroblastic leukemia cell lines show no erythropoietin receptors on the cell surface [23]. Since EEB cells do not have the megakaryocytic marker CD41 or platelet-peroxidase activity, they do not show megakaryocytic features. EEB cells show dim expression of CD117 and bright expression of both CD175s and CD235a. These features correspond to colony-forming unit-erythroid cells. The differential capacity of EEB cells is limited: they differentiated to benzidine-positive cells with the addition of δ-ALA and hemin. Neither TPA nor retinoic acid induced the differentiation of EEB cells to benzidine-positive cells, CD41-positive cells or myelomonocytic cells. The karyotype of EEB cells was normal and the cells had no P53 gene mutation, tandem duplication of the FLT3 gene, or FLT3 activation loop mutation. Since it seems that leukemic cell lines showing a normal karyotype are rare, it is necessary to perform chromosomal analysis of EEB cells in more detail. Moreover, molecular mechanisms of EEB cell growth remain to be clarified.

GL-2 was established as an antibody that reacts with an unbranched type 2 carbohydrate chain (i antigen). Thereafter, it was shown that GL-2 also reacts with a glycolipid, phosphatidylglucoside (PhGlc) [13]. Recently, GL-7, a recombinant Fab fragment of GL-2, has been prepared and shown to induce granulocytic differentiation of HL-60 cells [14]. Such granulocytic differentiation is associated with the rapid phosphorylation of Src family kinases, leading to an up- and down-regulation of CD38 and c-Myc expression, respectively. In our study, the binding of GL-2 to EEB cells was shown by flow cytometry and immunofluorescence microscopic analysis, respectively. We demonstrated that GL-7 induced production of HbF by EEB cells in a dose-dependent and a time-dependent manner. The accumulation of the γ-globin message in EEB cells treated with GL-7 was confirmed by quantitative real-time PCR analysis. These results suggest that GL-7 induces erythroid differentiation of EEB cells via the accumulation of γ-globin message. Since GL-2 binds both i antigen and PhGlc [12,13], glycolipid profiles of the EEB cell membrane were analyzed by TLC: EEB cells had PhGlc but not i antigen. Therefore, erythroid differentiation induced by GL-7 occurs via the interaction of GL-7 with PhGlc. Taken together, our results

and those of a previous study [14] suggest that PhGlc is involved in both myeloid and erythroid differentiation.

GL-7-mediated erythroid differentiation in EEB cells was found to be associated with apoptosis. This is not surprising: it is well known that erythroid differentiation of K562 cells is usually associated with terminal cell division [24,25]. Recently, Bianchi et al. demonstrated that tallimustine-mediated induction of erythroid differentiation of K562 cells is associated with apoptosis [26]. Tallimustine is a synthetic derivative of distamycin, which is a DNA-binding compound, and exhibits a very high level of anti-tumor activity [27]. Several antibodies cause the apoptosis of target cells: Rituximab, an anti-CD20 antibody, leads to direct signaling for apoptosis as well as complement activation and cell-mediated cytotoxicity in CD20-positive B cells [28], although it is not known whether the antibody induces lymphoid differentiation of the cells. Anti-carbohydrate monoclonal antibodies also induce apoptosis of target cells [14]: both DH59B, an anti-GM1 antibody, and Vj41, an anti-sphingomyelin antibody, induce apoptosis but not myeloid differentiation of HL-60 cells. GL-7-mediated erythroid differentiation of EEB cells may resemble tallimustine-mediated erythroid differentiation of K562 cells, because the two agents induce both erythroid differentiation and apoptosis in erythroid cells.

Glycosphingolipids are distributed in the outer leaf of the plasma membrane, forming clusters known as glycosphingolipid microdomains. The contribution of glycosphingolipid microdomains to signal transduction has been determined [29,30]: various ligands, including antibodies, toxins, lectins and complementary glycosphingolipids, bind to glycosphingolipid microdomains, leading to the activation or inhibition of transducer molecules associated with glycosphingolipids. Src-family kinases in the inner leaflet of glycosphingolipid microdomains can be activated via stimulation of surface glycosphingolipid microdomains. An anti-GM3 antibody inhibits Ras and MAP kinase activity, while it activates Rho and Lyn activity. Recently, it has been shown that PhGlc forms microdomains in HL60 cells [14]. The granulocytic differentiation of HL60 cells induced by GL-7 is associated with a rapid phosphorylation of Src family kinases [14]. Since GL-7 is a recombinant monovalent Fab fragment antibody, the granulocytic differentiation of HL60 cells induced by GL-7 does not depend on clustering of PhGlc like the interaction of galectin-1 and CD45 in T cells [31]. Therefore, PhGlc-mediated direct signaling leads to the granulocytic differentiation of HL60 cells via the phosphorylation of Src family kinases. In contrast, PhGlc-mediated erythroid differentiation in EEB cells was not associated with tyrosine phospholyration. PhGlc-mediated signaling may differ among cell lineages. EEB cells are useful for examining the association between signal transduction and erythroid differentiation mediated by PhGlc.

We showed that GL-2 reacted with erythroblasts developed from both adult bone marrow and cord blood but not with CD34-positive cells. Therefore, the i antigen and/or PhGLc might play a role both in fetal and in adult erythropoiesis.

In summary, the early erythroblastic leukemia cell line, EEB, was established from a patient with early erythroblastic leukemia. The cell line has a normal karyotype and retains erythroblastic features. The cell line can be available upon suitable request for further analysis.

Acknowledgements

The authors thank Dr. Eguchi for performing electron microscopic analysis, Dr. Inokuchi for performing gene mutation analysis, and technicians in Mitsubishi Kagaku Bio-Clinical Laboratories for performing multicolor FISH analysis.

References

[1] Tedder TF, Steeber DA, Chen A, Engel P. The selectins: vascular adhesion molecules. FASEB J 1995;10:866–73.
[2] McIntyre TM, Prescott SM, Weyrich AS, Zimmerman GA. Cell–cell interactions: leukocyte-endothelial interactions. Curr Opin Hematol 2003;10:150–8.
[3] Hakomori S. Possible role of glycolipid in development, cell growth regulation, and transformation. Prog Clin Biol Res 1980;41:873–86.
[4] Fukuda MN, Levery SB. Glycolipids of fetal, newborn, and adult erythrocytes: glycolipid pattern and structural study of H3-glycolipid from newborn erythrocytes. Biochemistry 1983;22:5034–40.
[5] Muroi K, Suda T, Nakamura M, Okada S, Nojiri H, Amemiya Y, et al. Expression of sialosyl-Tn in colony-forming unit-erythroid, erythroblasts, B cells, and a subset of CD4+ cells. Blood 1994;83:84–91.
[6] Muroi K, Amemiya Y, Sievers EL, Miura Y, Hakamori SI, Loken MR. Expression of sialosyl-T and disialosyl-T antigens in erythroid cells. Leuk Lymphoma 1997;25:403–14.
[7] Kannagi R, Papayannopoulou T, Nakamoto B, Cochran NA, Yokochi T, Stamatoyannopoulos G, et al. Carbohydrate antigen profiles of human erythroleukemia cell lines HEL and K562. Blood 1983;62:1230–41.
[8] Hakomori S. Tumor-associated carbohydrate antigens. Annu Rev Immunol 1984;2:103–26.
[9] Muroi K, Tarumoto T, Akioka T, Kirito K, Nagai T, Izumi T, et al. Sialyl-Tn- and neuron-specific enolase-positive minimally differentiated erythroleukemia. Intern Med 2000;39:843–6.
[10] Rowley PT, Ohlsson-Wilhelm BM, Farley BA, LaBella S. Inducers of erythroid differentiation in K562 human leukemia cells. Exp Hematol 1981;9:32–7.
[11] Eguchi M, Ozawa T, Sakakibara H, Sugita K, Iwama Y, Furukawa T. Ultrastructural and ultracytochemical differences between megakaryoblastic leukemia in children and adults. Analysis of 49 patients. Cancer 1992;70:451–8.
[12] Nagatsuka Y, Watarai S, Yasuda T, Higashi H, Yamagata T, Ono Y. Production of human monoclonal antibodies to i blood group by EBV-induced transformation: possible presence of a new glycolipid in cord red cell membranes and human hematopoietic cell lines. Immunol Lett 1995;46:93–100.
[13] Nagatsuka Y, Kasama T, Ohashi Y, Uzawa J, Ono Y, Shimizu K, et al. A new phosphoglycerolipid, 'phosphatidylglucose', found in human cord red cells by multi-reactive monoclonal anti-i cold agglutinin, mAb GL-1/GL-2. FEBS Lett 2001;497:141–7.
[14] Nagatsuka Y, Hara-Yokoyama M, Kasama T, Takekoshi M, Maeda F, Ihara S, et al. Carbohydrate-dependent signaling from

the phosphatidylglucoside-based microdomain induces granulocytic differentiation of HL60 cells. Proc Natl Acad Sci USA 2003;100:7454–9.
[15] Hoyer JD, Penz CS, Fairbanks VF, Hanson CA, Katzmann JA. Flow cytometric measurement of hemoglobin F in RBCs: diagnostic usefulness in the distinction of hereditary persistence of fetal hemoglobin (HPFH) and hemoglobin S-hPFH from other conditions with elevated levels of hemoglobin F. Am J Clin Pathol 2002;117:857–63.
[16] Shinjo K, Takeshita A, Higuchi M, Ohnishi K, Ohno R. Erythropoietin receptor expression on human bone marrow erythroid precursor cells by a newly-devised quantitative flow-cytometric assay. Br J Haematol 1997;96:551–8.
[17] Lee JY, Lee CH, Shim SH, Seo HK, Kyhm JH, Cho S, et al. Molecular cytogenetic analysis of the monoblastic cell line U937. karyotype clarification by G-banding, whole chromosome painting, microdissection and reverse painting, and comparative genomic hybridization. Cancer Genet Cytogenet 2002;137:124–32.
[18] Vermes I, Haanen C, Steffens-Nakken H, Reutelingsperger C. A novel assay for apoptosis. Flow cytometric detection of phosphatidylserine expression on early apoptotic cells using fluorescein labelled Annexin V. J Immunol Methods 1995;184: 39–51.
[19] Maeda F, Nagatsuka Y, Ihara S, Aotsuka S, Ono Y, Inoko H, et al. Bacterial expression of a human recombinant monoclonal antibody fab fragment against hepatitis B surface antigen. J Med Virol 1999;58:338–45.
[20] Ohmine K, Nagai T, Tarumoto T, Miyoshi T, Muroi K, Mano H, et al. Analysis of gene expression profiles in an imatinib-resistant cell line, KCL22/SR. Stem Cells 2003;21:315–21.
[21] Katsumata O, Hara-Yokoyama M, Sautes-Fridman C, Nagatsuka Y, Katada T, Hirabayashi Y, et al. Association of FcgammaRII with low-density detergent-resistant membranes is important for cross-linking-dependent initiation of the tyrosine phosphorylation pathway and superoxide generation. J Immunol 2001;167:5814–23.
[22] Miyazaki Y, Kuriyama K, Higuchi M, Tsushima H, Sohda H, Imai N, et al. Establishment and characterization of a new erythropoietin-dependent acute myeloid leukemia cell line, AS-E2. Leukemia 1997;11:1941–9.
[23] Drexler HG, Mastsuo AY, MacLeod RA. Continuous hematopoietic cell lines as model systems for leukemia-lymphoma research. Leuk Res 2000;24:881–911.
[24] Murate T, Kagami Y, Hotta T, Yoshida T, Saito H, Yoshida S. Terminal differentiation of human erythroleukemia cell line K562 induced by aphidicolin. Exp Cell Res 1990;191:45–50.
[25] Hatse S, Schols D, De Clercq E, Balzarini J. 9-(2-Phosphonylmethoxy-ethyl)adenine induces tumor cell differentiation or cell death by blocking cell cycle progression through the S phase. Cell Growth Differ 1999;10:435–46.
[26] Bianchi N, Chiarabelli C, Borgatti M, Mischiati C, Fibach E, Gambari R. Accumulation of gamma-globin mRNA and induction of erythroid differentiation after treatment of human leukaemic K562 cells with tallimustine. Br J Haematol 2001;113:951–61.
[27] Punt CJ, Humblet Y, Roca E, Dirix LY, Wainstein R, Polli A, et al. Tallimustine in advanced previously untreated colorectal cancer, a phase II study. Br J Cancer 1996;73:803–4.
[28] Cragg MS, Glennie MJ. Antibody specificity controls in vivo effector mechanisms of anti-CD20 reagents. Blood 2004;103:2738–43.
[29] Hakomori S, Yamamura S, Handa AK. Signal transduction through glyco(sphingo) lipids. Introduction and recent studies on glyco (sphingo) lipid-enriched microdomains. Ann NY Acad Sci 1998;845:1–10.
[30] Kasahara K, Sanai Y. Functional roles of glycosphingolipids in signal transduction via lipid rafts. Glycoconj J 2000;17:153–62.
[31] Nguyen JT, Evans DP, Galvan M, Pace KE, Leitenberg D, Bui TN, et al. CD45 modulates galectin-1-induced T cell death: regulation by expression of core 2 O-glycans. J Immunol 2001;167:5697–707.

THE JOURNAL OF GENE MEDICINE
J Gene Med 2006; **8**: 990–997.
Published online 10 May 2006 in Wiley InterScience (www.interscience.wiley.com) **DOI:** 10.1002/jgm.916

RESEARCH ARTICLE

Utility of intraperitoneal administration as a route of AAV serotype 5 vector-mediated neonatal gene transfer

Tsuyoshi Ogura,[1,3] Hiroaki Mizukami,[1]* Jun Mimuro,[2] Seiji Madoiwa,[2] Takashi Okada,[1] Takashi Matsushita,[1] Masashi Urabe,[1] Akihiro Kume,[1] Hiromi Hamada,[3] Hiroyuki Yoshikawa,[3] Yoichi Sakata,[2] Keiya Ozawa[1]*

[1]*Division of Genetic Therapeutics, Center for Molecular Medicine, Jichi Medical School, Tochigi, Japan*

[2]*Division of Cell and Molecular Medicine, Center for Molecular Medicine, Jichi Medical School, Tochigi, Japan*

[3]*Department of Obstetrics and Gynecology, Institute of Clinical Medicine, Graduate School of Comprehensive Human Sciences, University of Tsukuba, Ibaraki, Japan*

*Correspondence to: Hiroaki Mizukami and Keiya Ozawa, Division of Genetic Therapeutics, Jichi Medical School, 3311-1 Yakushiji, Minamikawachi-machi, Kawachi-gun, Tochigi 329-0498, Japan.
E-mail: miz@jichi.ac.jp; kozawa@ms2.jichi.ac.jp

Received: 23 September 2005
Revised: 14 February 2006
Accepted: 22 February 2006

Abstract

Background Gene transfer into a fetus or neonate can be a fundamental approach for treating genetic diseases, particularly disorders that have irreversible manifestations in adulthood. Although the potential utility of this technique has been suggested, the advantages of neonatal gene transfer have not been widely investigated. Here, we tested the usefulness of neonatal gene transfer using adeno-associated virus (AAV) vectors by comparing the administration routes and vector doses.

Methods To determine the optimal administration route, neonates were subjected to intravenous (*iv*) or intraperitoneal (*ip*) injections of AAV5-based vectors encoding the human coagulation factor IX (*hfIX*) gene, and the dose response was examined. To determine the distribution of transgene expression, vectors encoding *lacZ* or luciferase (*luc*) genes were used and assessed by X-gal staining and *in vivo* imaging, respectively. After the observation period, the vector distribution across tissues was quantified.

Results The factor IX concentration was higher in *ip*-injected mice than in *iv*-injected mice. All transgenes administered by *ip* injection were more efficiently expressed in neonates than in adults. The expression was confined to the peritoneal tissue. Interestingly, a sex-related difference was observed in transgene expression in adults, whereas this difference was not apparent in neonates.

Conclusions AAV vector administration to neonates using the *ip* route was clearly advantageous in obtaining robust transgene expression. Vector genomes and transgene expression were observed mainly in the peritoneal tissue. These findings indicate the advantages of neonatal gene therapy and would help in designing strategies for gene therapy using AAV vectors. Copyright © 2006 John Wiley & Sons, Ltd.

Keywords AAV vector; neonatal gene therapy; luciferase; coagulation factor IX

Introduction

Due to its unique properties, the adeno-associated virus (AAV) vector is one of the most promising vehicles for gene therapy. It can efficiently transduce a variety of tissues, and long-term transgene expression can be attained. Therefore, the AAV vector is suitable for supplemental gene therapy, particularly for hemophilia. However, despite the promising results obtained in animals [1–4], insignificant levels of human coagulation factor IX (hFIX)

were observed in humans after intramuscular (*im*) injection of the AAV vector [5,6]. The use of alternative serotypes may possibly improve the therapeutic outcome. To achieve therapeutic levels of hFIX expression, several reports have suggested the necessity of optimizing the serotypes of the AAV vector for each administration route [7–10].

It is also believed that neonatal or fetal gene therapy is potentially useful for improving the therapeutic outcome of genetic diseases. These methods are advantageous for preventing early manifestations of genetic diseases, for transducing organ systems that are not easily accessible in later life [11–13], and for providing robust transgene expression at relatively low vector doses. Moreover, since the neonatal and fetal immune systems are immature, gene transfer during this period may induce tolerance to transgene products [7,14,15].

With regard to the utility of the AAV serotypes for neonatal gene therapy, relatively little information is currently available. Limited utility of the AAV serotype 2 (AAV2) vector for *in utero* gene transfer was previously described [16]. It was reported that an intraperitoneal (*ip*) injection of AAV5-based vectors resulted in transgene expression that is at least 10 times higher than that obtained with an *ip* injection of the AAV2 vector [17]. In this study, based on these reports and our previous observations that demonstrated the advantages of AAV5 in gene transfer experiments [18,19], we compared the efficacy and distribution of transgene expression for evaluating the utility of AAV5-based vectors administered to neonates and adult mice either by an *ip* or intravenous (*iv*) injection.

Materials and methods

Plasmids and AAV vectors

Plasmids for AAV vector production were purchased from Stratagene (La Jolla, CA, USA). pAAV5-CMV-LacZ, a plasmid encoding LacZ, and 5RepCapA, a helper plasmid, were donated by Dr. J. A. Chiorini (National Institutes of Health, Bethesda, MD, USA). pAAV5-CMV-hFIX that contains the hFIX sequence was prepared as previously described [20,21], with the inverted terminal repeat (ITR) sequences changed to those of the AAV5 vector. pAAV5-CMV-Luc, which harbors the firefly luciferase gene, was originally purchased from Promega (Madison, WI, USA), and its ITR sequences were also changed to those of the AAV5 vector. Recombinant AAV vector stocks were prepared in accordance with an adenovirus-free triple-plasmid transfection protocol [22]. After harvest, vector solutions were purified twice on a cesium chloride (CsCl) gradient and quantified by DNA dot blot hybridization. The same vector stock was used in the same series of experiments in order to minimize the variability that could occur due to the potential differences in vector potency.

Animal procedures

All animal experiments were performed in accordance with the standards in the Guide for the Care and Use of Laboratory Animals (NIH Publication No. 85-23) and the institutional guidelines. Pregnant female C57BL/6 mice were purchased from CLEA Japan, Inc. (Hamamatsu, Japan), and the neonates were subjected to vector injection within 24 h of birth. Isoflurane anesthesia was applied at the time of injection, and the injection volume was kept constant at 20 μl throughout the study. In order to determine a suitable route for administration in neonates, the AAV5-CMV-hFIX vector was injected either intravenously (*iv*, into the jugular vein) or intraperitoneally (*ip*). In order to validate the usefulness, *ip* injections of the AAV5-CMV-hFIX vector at higher doses were tested. In order to assess the tissue distribution of the vector and transgene expression, the AAV5-CMV-LacZ vector ($n = 8$) or the AAV5-CMV-Luc vector ($n = 10$) was injected into the peritoneal cavity. Along with the neonates, an adult group comprising 12-week-old mice were used as adults for *ip* injection, and the AAV5-CMV-hFIX vector ($n = 8$), AAV5-CMV-LacZ vector ($n = 6$), or AAV5-CMV-Luc vector ($n = 10$) was administered. All procedures were performed safely, and animal death was rarely observed following vector injection.

Determination of the plasma concentration of human factor IX

Whole blood was collected from the tail vein by using heparinized capillary tubes. Plasma concentrations of the hFIX protein were determined as described previously [21]. The detection limit of this assay was 1 ng/ml. Normal human plasma stock was used as the standard. This assay system did not react with murine factor IX [21].

Detection and quantitation of vector genomes

Organs were isolated from mice after 16 weeks of vector injection. Tissue samples were frozen in liquid nitrogen and stored at −70 °C. Total DNA was extracted from the tissue samples using the DNeasy tissue kit (Qiagen GmbH, Hilden, Germany). In order to analyze the vector distribution following *ip* administration, total DNA was extracted from various tissues and subjected to quantitative polymerase chain reaction (Q-PCR) using an ABI PRISM 7900HT (Applied Biosystems, Foster City, CA, USA), under conditions that were previously described [23]. The detection limit was 0.01 vector genome copies per diploid genome equivalent (g.c./d.g.e.).

Histochemistry

The mice were sacrificed, and each tissue was obtained at 8 or 10 weeks after the AAV5-CMV-LacZ injection. For microscopic evaluation, the tissues were washed, incubated with phosphate-buffered saline (PBS) containing sucrose (15–30%), frozen in OTC compound (Tissue Tek, Miles Inc., Elkhart, IN, USA) in dry ice/ethanol, attached to polylysine-coated glass slides, and analyzed by standard X-gal staining [24].

Bioluminescence studies

For *in vivo* bioluminescence imaging, the mice were anesthetized with isoflurane, and an aqueous solution of luciferin substrate (150 μg/10 μl/g body weight) was injected into the intraperitoneal cavity 12 min prior to imaging. The mice were placed in a light-tight chamber to maintain complete darkness. Photons transmitted through the tissues were then collected and analyzed using IVIS Imaging Systems and Living Image software (Xenogen Corp., Alameda, CA, USA). Imaging was performed with 5 s of the integration time. The range of the reference pseudocolor scale, representing the light intensity, was kept constant for all mice. For *ex vivo* luciferase analysis, in order to discontinue the follow up of the *in vivo* observation, the representative mice were chosen and sacrificed 10 min after *ip* injection of the luciferin substrate solution (150 μg/10 μl/g body weight), and the internal organs were then separated. Each organ was immediately placed into each well of a 24-well dish containing 1 : 50 dilutions of an aqueous solution of the luciferin substrate (final concentration, 300 μg/ml), and bioluminescence was measured using 60 s of the integration time. The light intensity was calculated based on the weight of the tissue.

Statistical analysis

All data are shown as means ± standard deviation (SD). To compare the means between the two groups, statistical analysis was performed by applying Student's *t* test after confirming the equality between the variances of the groups. If the variances were unequal, Mann-Whitney *U* tests were performed. Values of $p < 0.05$ were regarded to be significant.

Results

Comparison of delivery routes for neonatal injection

As shown in Figure 1A, the plasma levels of hFIX were higher in the *ip*-injected group than in the *iv*-injected group. The plasma concentration of hFIX at 8 weeks for the two groups was 21.8 ± 5.0 ng/ml and 10.2 ± 3.1 ng/ml, respectively, and the difference in the hFIX concentration was significant after 6 weeks ($p < 0.01$).

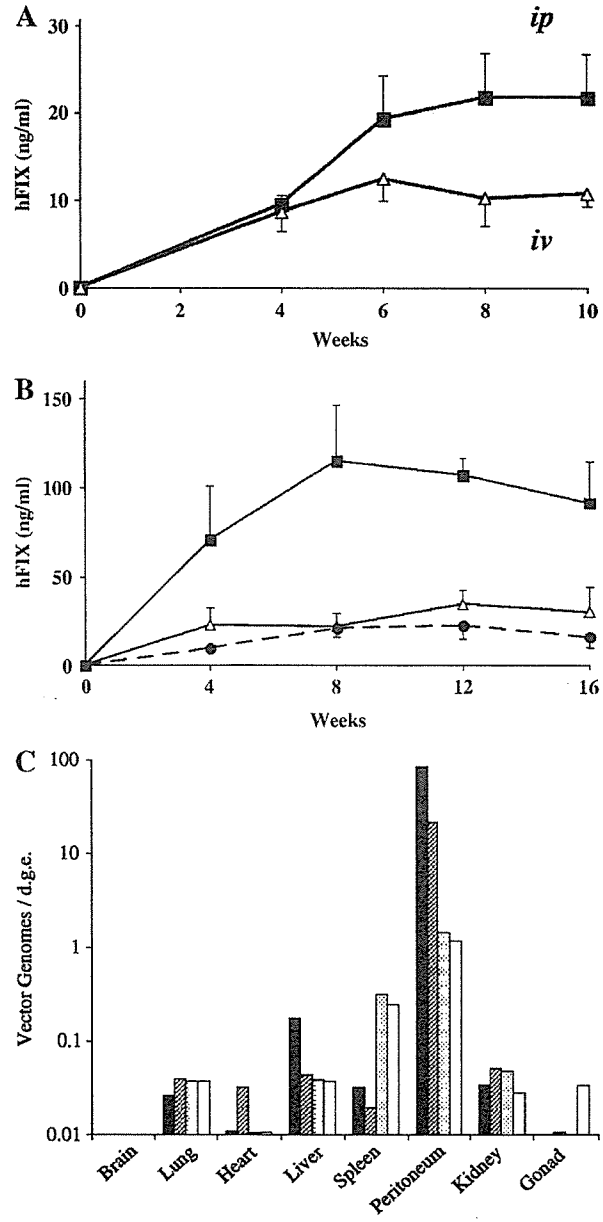

Figure 1. Analysis of C57BL/6 mice after intraperitoneal (*ip*) or intravenous (*iv*) injection of AAV vectors. (A) Plasma hFIX concentration after *ip* (n = 4, closed squares) and *iv* (n = 5, open triangles) administration of the AAV5-CMV-hFIX vector (1×10^{10} genome copies/body weight (g.c./g)) in the C57BL/6 neonatal mice. (B) Plasma hFIX concentration in neonatal mice after *ip* injections at different vector doses. The vector dose was 1×10^{10} g.c./g (closed circles), 3×10^{10} g.c./g (open triangles), or 3×10^{11} g.c./g (closed squares). (C) The number of vector genomes within the tissues at 10 weeks after *ip* injection into neonates. Total DNA (100 ng) was analyzed by Q-PCR, and the results were calculated as vector genomes per diploid genome equivalent (d.g.e.). Closed, hatched, dotted, and open columns indicate the results with neonatal males, neonatal females, adult males, and adult females, respectively

Effect of the vector dose in *ip* administration

As *ip* administration appeared to be more promising than *iv*, we focused on the utility of *ip* in neonates. For this purpose, increasing doses of AAV5-CMV-hFIX vectors were tested. Higher hFIX concentrations were observed in animals with higher vector doses (Figure 1B). In the group with the highest vector dose (3×10^{11} genome copies/body weight (g.c./g)), the plasma hFIX concentrations were approximately 100 ng/ml, which is a therapeutically relevant level for severe hemophilia B, and these concentrations were sustained throughout the observation period.

Tissue distribution of the AAV vector genome

The tissue distribution of the vector genome after the *ip* injection into male mice was analyzed by real-time PCR. Substantial numbers of vector genomes were detected in the peritoneum and to a lesser extent in the liver and other tissues (Figure 1C). Note that the vector genomes are shown on a logarithmic scale.

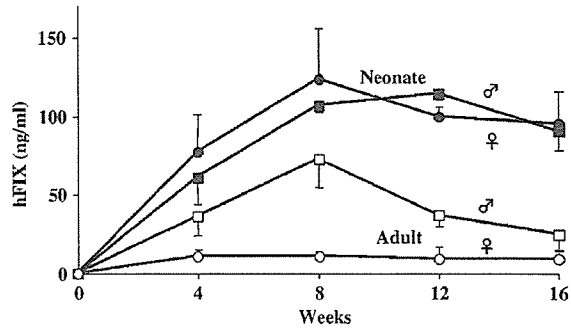

Figure 2. Plasma hFIX concentrations in mice after *ip* injections into different groups. The AAV5-CMV-hFIX vector at a dose of 3×10^{11} g.c./g was injected into C57BL/6 neonatal males (n = 6, closed squares), neonatal females (n = 4, closed circles), adult males (n = 4, open squares), and adult females (n = 4, open circles)

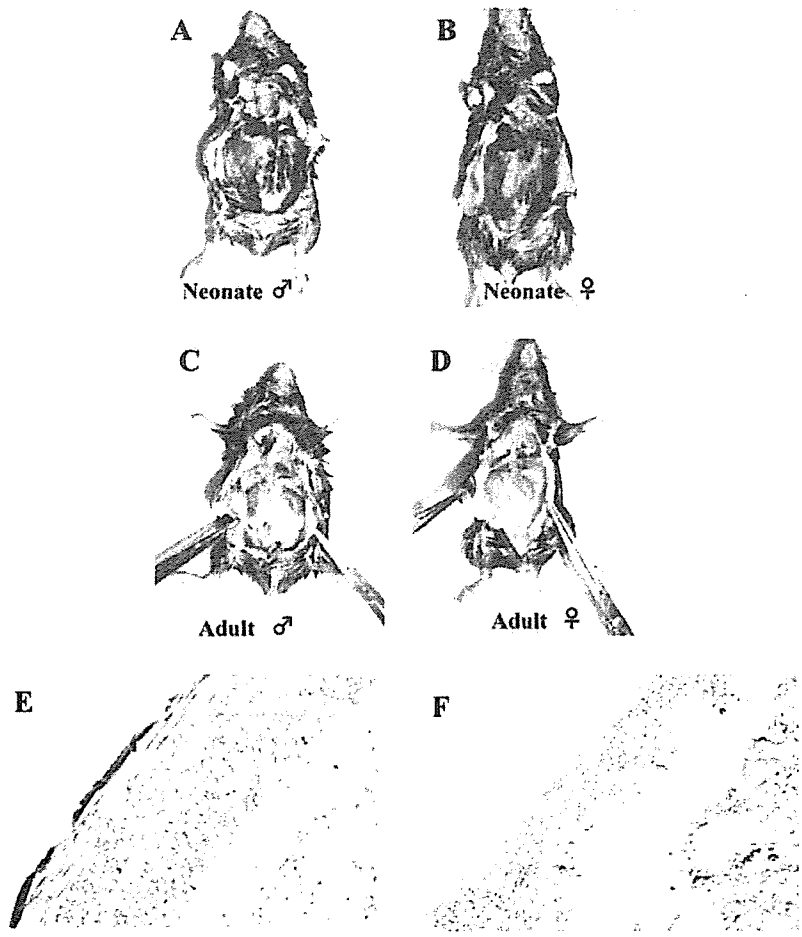

Figure 3. β-Galactosidase expression at 8 weeks after *ip* injection of the AAV5-CMV-LacZ vector at a dose of 1×10^{11} g.c./g in the C57BL/6 mice (A–D). X-gal staining was performed after removal of the intraperitoneal organs. Histochemistry with β-galactosidase performed on tissues from the neonatal male peritoneum after the injection stained the mesothelium (E) and the untransduced control (F) (final magnification ×100)

J Gene Med 2006; 8: 990–997.
DOI: 10.1002/jgm

Influence of sex and age of mice on transgene expression

In order to compare the efficiency with regard to the sex and age of mice during administration, the same dose of the AAV vector based on the body weight (3×10^{11} g.c./g) was administered by *ip* injection to both neonatal and adult mice. As summarized in Figure 2, the plasma levels of hFIX were significantly higher in males than in females when adults were used ($p < 0.05$). On the other hand, there were no sex-related differences in the hFIX concentration in neonates. Moreover, the hFIX levels were much higher in neonates (neonate vs. adult; $p < 0.05$ in males, $p < 0.01$ in females). After 8 weeks, a considerable reduction in the plasma hFIX concentration was observed in adult males.

Tissue distribution of transgene expression following *ip* injection

To evaluate the efficacy and location of transgene expression following *ip* vector administration, 1×10^{11} g.c./g of the AAV5-CMV-LacZ vector was injected into either neonatal or adult mice. After 8 weeks, the mice were sacrificed and their tissues were subjected to X-gal staining. As shown in Figures 3A–3D, β-galactosidase expression was observed in the peritoneum. Robust β-galactosidase expression was observed in both male and female mice in the neonatal group (Figures 3A and 3B). In contrast, in the injected adults, only weak β-galactosidase expression was observed in the male mice, and faint expression was detected in the female mice (Figures 3C and 3D). Other tissues were also analyzed by X-gal staining, and none of these, including liver and kidney, showed positive results (data not shown). Microscopic examination of the peritoneum of neonatally injected male mice revealed β-galactosidase expression in mesothelial cells, while the control mice did not show X-gal positivity (Figures 4E and 4F).

In vivo and *ex vivo* analysis using bioluminescence

To quantify the distribution of transgene expression, the AAV5-CMV-Luc vectors were administered *ip* to neonatal and adult mice at an equivalent vector dose based on the body weight (3×10^9 g.c./g). Luciferase expression was observed by *in vivo* bioluminescence imaging 10 weeks after the vector injection (Figures 4A–4D). Quantitative results of *in vivo* bioluminescence are shown in Figure 4E. In neonates, no sex-related difference was found in luciferase expression ($3.8 \times 10^9 \pm 1.2 \times 10^8$ photons/s and $2.9 \times 10^9 \pm 1.0 \times 10^9$ photons/s for the males and females, respectively, $p = 0.13$). In contrast, a significant difference in distribution and quantitation was observed in adults ($1.3 \times 10^9 \pm 7.2 \times 10^8$ photons/s and $5.3 \times 10^7 \pm 1.6 \times 10^7$ photons/s for males and females, respectively, $p < 0.05$). In order to identify the tissues responsible for luciferase expression, an *ex vivo* bioluminescence analysis was performed at 10 weeks after the vector injection; this demonstrated that the luciferase expression was localized in the peritoneum (Figure 5A). As shown on the pseudocolor scale, the white color showed background of the assay and did not reflect luciferase expression. A luminometric analysis of individual tissues from representative animals revealed a difference in the expression in the peritoneum among the injected neonates and adults (3.1×10^8 and 1.6×10^8 photons/s/g for male and female neonates, respectively; 1.1×10^8 and 7.9×10^4 photons/s/g for male and female adults, respectively) (Figure 5B).

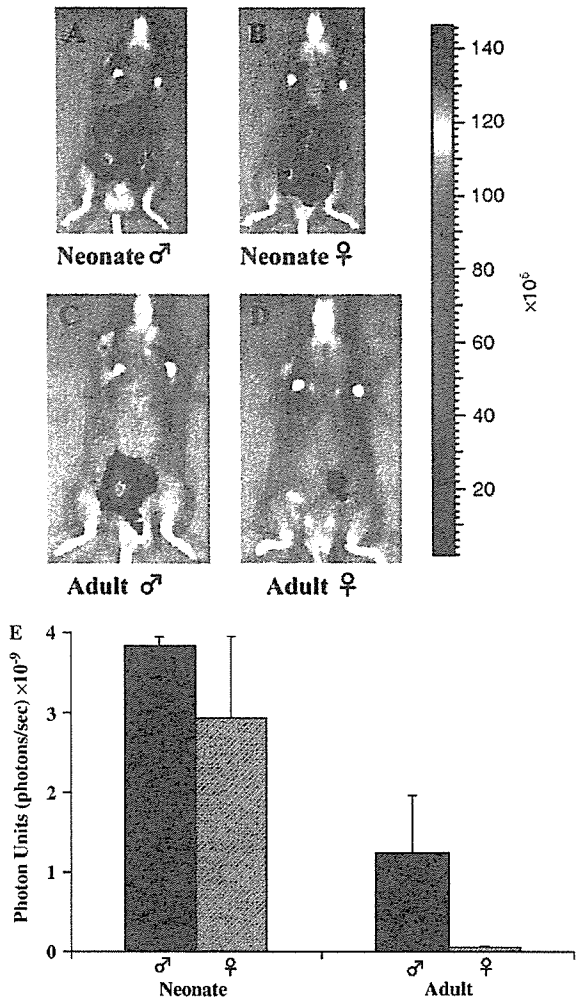

Figure 4. *In vivo* **bioluminescence imaging at 10 weeks after** *ip* **injection of the AAV5-CMV-Luc vector at a dose of 5 x 10^9 g.c./1.5 g in the C57BL/6 mice (A–D). Images were analyzed under the same condition, and the reference color bar, indicating the photon units (photons/s), is the same for all mice. (E) Quantitative results of** *in vivo* **bioluminescence imaging in neonatal males (n = 6, closed columns) and females (n = 4, hatched column), and adult males (n = 5, dotted column) and females (n = 5, open column), are shown. Mice were transduced with 5 x 10^9 g.c./1.5 g of the AAV5-CMV-Luc vector (2.5 x 10^8 g.c./μl). The ordinate indicates the photon units (photon/s)**

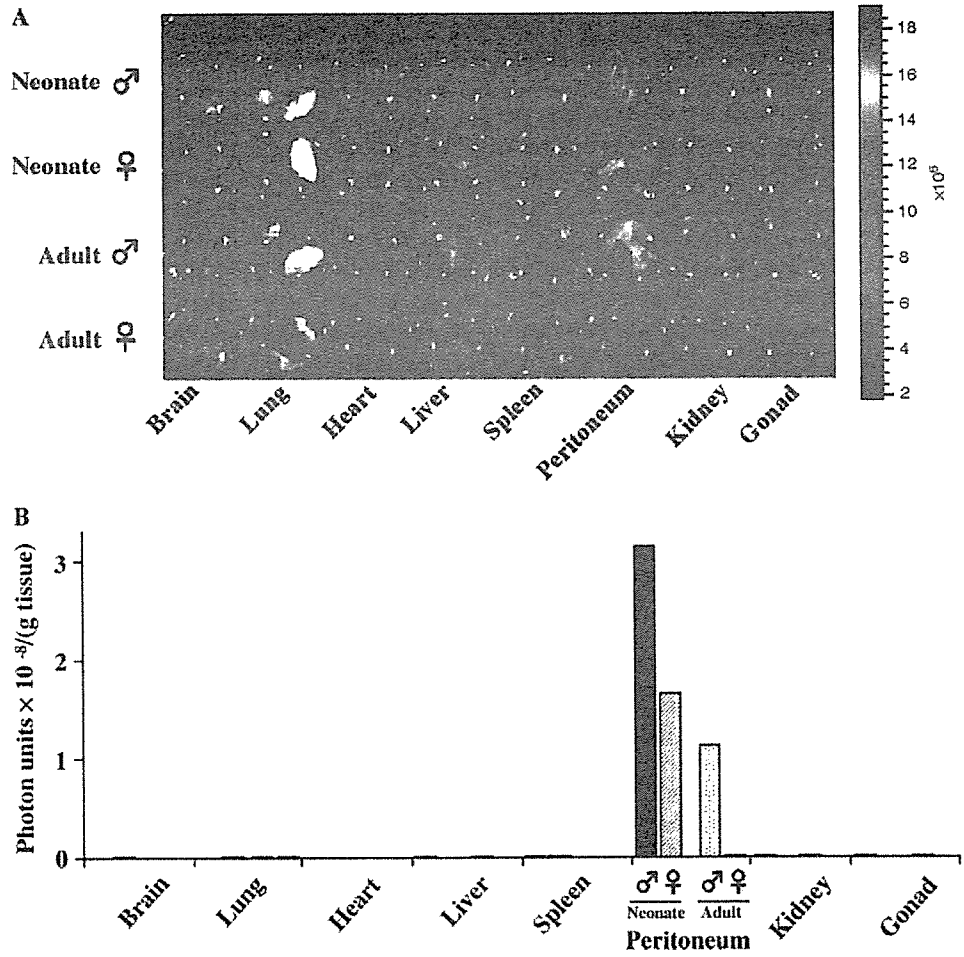

Figure 5. Analysis of tissue-specific expression after *ip* injection of the AAV5-CMV-Luc vector. (A) *Ex vivo* bioluminescence images of injected neonates and adults are shown. Mice were sacrificed at 10 weeks after vector injection and the major organs were extracted and placed into each well of a 24-well dish containing luciferin substrate solution in order to measure the individual bioluminescence. (B) Quantitative results of transgene expression are as indicated in (A). The ordinate shows the photon units (photons/s)

Discussion

In this study, we tested the utility of neonatal gene transfer by using AAV5-based vectors. All genes tested – *lacZ*, *hfIX*, and *luc* – demonstrated robust transgene expression after *ip* injection. The advantage of neonatal gene transfer was clearly demonstrated by the plasma hFIX levels after injecting both adult and neonatal mice with equivalent doses of the AAV-CMV-hFIX vector (3×10^{11} g.c./g). Throughout the observation period, a higher hFIX concentration was detected in neonates than in adults; therapeutic levels of hFIX were maintained even after maturation (Figure 2). Another comparison using vectors encoding luciferase at an equivalent vector dose also resulted in a higher transgene expression in neonates (Figure 4). These data support the advantages of neonatal gene transfer.

Neonatal gene delivery in mice is technically difficult due to their size. In this study, we demonstrated the usefulness of *ip* injections as a route of vector delivery. On the other hand, we did not include the *im* route in this series of experiments because the injection volume was strictly limited in neonates. However, this latter method is apparently an attractive route of administration in clinical applications. Therefore, the efficacy of *im* administration requires further analysis in larger animal models.

In this study, transgene expression was mostly confined to the peritoneum after *ip* injection into neonates. This was confirmed by different modes of detection. In addition, the vector genome distribution was mostly comparable to the level of transgene expression. However, in a previous report, transgene expression was also observed in tissues other than the peritoneum when fetuses were injected [17]. Since the vector system and the promoter were the same, the difference in tissue distribution may be related to the age at the time of injection, vector dose, technical details, or other unrecognized factors. At present, the mechanism responsible for tissue specificity is not clear. The abundance of receptor molecules, such as platelet-derived